Crime Modeling with Lévy Flights

Sorathan Chaturapruek, Jonah Breslau, Daniel Yazdi,
Theodore Kolokolnikov, and Scott G. McCalla

October 21, 2012

Abstract

The UCLA burglary hotspot model, introduced in [Short et.al., Math. Models. Meth. Appl. Sci., 18, Suppl. (2008), pp. 1249–1267], models the formation of hotspots of criminal activity. In this paper, we extend the UCLA model to incorporate a more realistic model of human locomotion. The movement of the criminal agents follows a biased Lévy flight with step-sizes distributed according to a power-law distribution. The biased Brownian motion of the original model is then derived as a special case. Starting with an agent-based model, we derive its continuum limit. This consists of two equations and involves the fractional Laplacian operator. A numerical method based on the Fast Fourier transform is used to simulate the continuum model; these simulations compare favorably with the direct numerical simulations of the agent-based model. A Turing-type analysis is performed to estimate how the instability of the homogeneous steady state, as well as the expected number of hotspots, depends on the system parameters and especially the exponent of the underlying power law. The assumptions of the underlying agent-based model naturally lead to a separation of scales of the diffusion coefficients in the continuum limit. Using these assumptions, we asymptotically construct the leading-order profile of the localized hotspot of criminal activity.

Keywords: fractional Laplacian, super-diffusion, hotspots, Lévy flights, crime modeling, Turing analysis

1 Introduction

Crime is an unfortunate but persistent part of life in all parts of the world. Furthermore, it is not uniformly distributed; certain neighborhoods contain high levels of criminal activity in comparison to others. This can be due to socioeconomic forces, geographical structure, or even the composition of the local businesses [3, 5, 10, 23, 1, 4, 25, 32, 33, 16, 21]. Surprisingly, localized regions of unusually high crime can also occur as a result of previous crimes in the area [8, 17, 30, 22]. These regions containing elevated criminal activity are known as hotspots. In a series of pioneering works [28, 29, 27, 30], the UCLA group has proposed a mathematical model (henceforth referred to as the *UCLA model*) for understanding the dynamics of criminal activity. For simplicity, they focused on residential burglaries wherein the targets are stationary. Only the offender's movements need to be understood.

The UCLA model [28] incorporates the empirically observed phenomena of repeat/near-repeat events and the "broken windows" effect [34]. Repeat and near-repeat events refer to the self-exciting nature of burglary. For a short time after a home is robbed, it becomes a more likely target for another burglary within the next few weeks; this is a repeat event. Additionally, the adjacent and nearby houses also become more likely targets for a future robbery; this is a near-repeat event. This

effect is clearly seen in the burglary data, and even the temporal and spatial decay of the increased robbery likelihood can be observed [8, 17, 30, 18, 15]. Once a thief has successfully burgled a home, the thief knows how to break in, how to navigate the neighborhood, and what other valuables are available to steal [30, 35]. A great deal of research has been done to understand this phenomenon [9, 15, 2, 31, 26, 7, 18]. The "broken windows" effect accounts for the diffusive nature of crime. Neighborhoods with high crime exude a sense of lawlessness, and a notion of crime tolerance. As a result, such neighborhoods can become more desirable targets for burglars.

Another assumption of the UCLA model is that criminals travel through space according to a random walk biased towards attractive burglary cites. In a discrete setting, this amounts to criminals moving only to adjacent homes with each time step, or in a continuous setting, spreading according to a biased diffusion. Under this assumption, burglars only have access to a single mode of transportation and have knowledge that is restricted to the homes directly adjacent to them. This assumption is expected to be an oversimplification for human motion. It has been argued that animal movements, including humans, generate Lévy flights instead of random walks [11, 24, 14, 6]. A Lévy flight enables an animal to more efficiently explore its territory for resources than a random walk. Instead of restricting movement only to neighboring sites, Lévy flghts exhibit long range jumps. The probability of a long jump is dictated by a power law distribution, and Brownian motion is equivalent to a Lévy flight with sufficiently strong decay in the distribution. These occasional long jumps interspersed with a local random walk can be seen in a typical daily commute in a big city. A commuter may first walk to bus which takes a "flight" to a different part of the city; the commuter then resumes walking to work, perhaps detouring to grab a coffee. The non-local nature of this motion allows criminals to more efficiently examine the space for potential homes to rob, but it also assumes the criminals have knowledge extending far beyond their immediate surroundings.

The goal of this paper is to extend the UCLA model to incorporate the "non-local" movement of criminals. The diffusion of attractiveness for burglary sites can be extracted from the data. Unfortunately, the movements of criminals is not tracked and cannot easily be found experimentally. We will specifically focus on motion by Lévy flights biased towards attractive burglary sites because they produce the well-known fractional Laplacian operator in the continuous limit. As in the original UCLA model [28], we start with an agent-based cellular automata model; this is derived in section §2. By taking the continuum limit, we obtain a system of two PDE's for the criminal density and the attractiveness field. Unlike the original model, the resulting PDE for the criminal density is nonlocal, whereas the equation describing the attractiveness field remains local. Specifically, the new model contains the fractional Laplacian, a non-local extension of the normal Laplacian, which allows for the super-diffusion of criminals. We perform a linear stability analysis (Turing analysis) around a homogeneous crime steady state and supplement this with numerical simulations that illustrate the effect of non-locality on hotspot formation. We find that increasing the non-locality can either increase the number of hotspots or decrease it, depending on the parameter regime. Additionally, it can stabilize or destabilize the homogeneous steady state. We conclude our study with an asymptotic construction of the hotspot profile under criminal Lévy flights in a singular regime.

2 Modeling biased Lévy flights

In this section, we derive a modified version of the UCLA model to incorporate the criminal motion based on biased Lévy flights. We begin with a review of the original agent-based model from [28]. We start with a cellular automata model where the burglars are located along a one-dimensional grid with grid spacing l. We define an "attractiveness field" $A_k(t)$ for each grid location k and time t. This can be decomposed into a static background term A_0 plus a dynamic term $B_k(t)$

$$A_k(t) \equiv A^0 + B_k(t). \tag{1}$$

In addition, we let $N_k(t)$ denote the number of criminals at each location k and time t. The evolution of the dynamic attractiveness term is modeled following [28] as

$$B_k(t+\delta t) = \left[(1-\hat{\eta})\, B_k(t) + \frac{\hat{\eta}}{2}\left(B_{k-1} + B_{k+1}\right)\right](1 - w\delta t) + \delta t A_k N_k \theta. \tag{2}$$

Here, δt is a characteristic time scale, $\frac{\hat{\eta}}{2}\left(B_{k-1} + B_{k+1}\right)$ represents the "broken windows" effect whereby the attractiveness of a given area is affected by the attractiveness of its neighbors, and $0 < \hat{\eta} < 1$ is the strength of this effect. The parameter w represents the decay rate of the dynamic attractiveness field. The term $\delta t A_k N_k$ is the mass-action law; it represents the total number of burglaries that took place in the time interval $[t, t+\delta t]$. θ is the proportionality constant.

Lévy flights represent a random motion whereby a particle takes steps whose distribution obeys a power law. For criminal motion, these steps should be biased towards areas with a high attractiveness A. Thus we define the relative weight of a criminal moving from point i to point k, where $i \neq k$, as

$$w_{i\to k} = \frac{A_k}{l^\mu \left|i-k\right|^\mu}. \tag{3}$$

Here μ is the exponent of the underlying power law for the Lévy Flight. The key feature is that the weight includes the attractiveness field A. The transition probability of a criminal moving from point i to point k, where $i \neq k$, is then given by

$$q_{i\to k} = \frac{w_{i\to k}}{\sum_{j\in\mathbb{Z}, j\neq i} w_{i\to j}}. \tag{4}$$

As in [28], we assume that the burglars obey the following simple rules: during the time interval δt, the burglar either commits a crime with probability $A_i \delta t$ or else moves on according to a biased flight; new criminals appear with rate Γ. These rules for the criminal population are encoded as

$$N_k(t+\delta t) = \sum_{i\in\mathbb{Z}, i\neq k} N_i \cdot (1 - A_i \delta t) \cdot q_{i\to k} + \Gamma \delta t. \tag{5}$$

We now take the continuum limit for $\delta t, l \ll 1$. Let $N(x,t) = N_k(t)$ where $x = kl$. Similarly define $A(x,t)$ and $B(x,t)$ such that (2) becomes

$$A(x,t+\delta t) - A_0 = \left[(1-\hat{\eta})\, A(x,t) + \frac{\hat{\eta}}{2}\left(A(x-l,t) + A(x+l,t)\right)\right](1 - w\delta t) + \delta t A N \theta. \tag{6}$$

Using a Taylor expansion and keeping only the leading order terms, we find the equation

$$A_t = \frac{l^2 \hat{\eta}}{2\delta t} A_{xx} - w(A - A_0) + AN\theta. \tag{7}$$

Due to the nonlocal criminal movement, the derivation of the continuum limit for N is more involved. We define

$$z := 2\sum_{k=1}^{\infty}\frac{1}{k^{\mu}} = 2\zeta(\mu) \text{ and} \tag{8}$$

$$\mathcal{L}f_i := \sum_{j\in\mathbb{Z},j\neq i}\frac{f_j - f_i}{|j-i|^{\mu}\, l^{\mu}}. \tag{9}$$

Additionally, we write

$$\begin{aligned}\sum_{j\in\mathbb{Z},j\neq i} w_{i\to j} &= \sum_{j\in\mathbb{Z},j\neq i}\frac{A_j - A_i}{l^{\mu}\,|i-j|^{\mu}} + \sum_{j\in\mathbb{Z},j\neq i}\frac{A_i}{l^{\mu}\,|i-j|^{\mu}}\\ &= A_i l^{-\mu} z + \mathcal{L}A_i\end{aligned}$$

so that

$$q_{i\to k} \sim \frac{A_k}{|i-k|^{\mu}}\left(\frac{1}{zA_i} - \frac{\mathcal{L}A_i l^{\mu}}{A_i^2 z^2}\right). \tag{10}$$

We then have

$$\frac{N_k(t+\delta t) - N_k(t)}{\delta t} = \frac{1}{\delta t}\left(\sum_{i\in\mathbb{Z},i\neq k} N_i(1 - A_i\delta t)q_{i\to k} - N_k\right) + \Gamma \tag{11}$$

and expand to find

$$\begin{aligned}\sum_{i\in\mathbb{Z},i\neq k} N_i(1-A_i\delta t)q_{i\to k} - N_k &= \sum_i N_i\,(1-A_i\delta t)\,\frac{A_k}{|i-k|^{\mu}}\left(\frac{1}{zA_i} - \frac{\mathcal{L}A_i l^{\mu}}{A_i^2 z^2}\right) - N_k\\ &\sim A_k\sum_i\left[\frac{\frac{N_i}{A_i} - \frac{N_k}{A_k}}{|i-k|^{\mu}\, z} - \frac{N_i}{|i-k|^{\mu}}\left(\frac{\mathcal{L}A_i l^{\mu}}{A_i^2 z^2}\right) - \delta t\frac{N_i}{|i-k|^{\mu}\, z}\right]\\ &\sim A_k\left[\frac{l^{\mu}}{z}\mathcal{L}\left(N_k/A_k\right) - N_k\frac{\mathcal{L}A_k l^{\mu}}{A_k^2 z} - \delta t N_k\right].\end{aligned}$$

The operator $\mathcal{L}$ can be approximated as

$$\mathcal{L}A_k \sim \frac{1}{l}\int_{-\infty}^{\infty}\frac{A(y) - A(x)}{|y-x|^{\mu}}dy \tag{12}$$

where $x = kl$ and $A_k \sim A(x)$. Next we write this operator in terms of the fractional Laplacian. We use the following definition of the fractional Laplacian in dimension d, from [20]:

$$-(-\Delta)^s f(x) := C_{d,2s}\int_{y\in\mathbb{R}^d}\frac{f(x) - f(y)}{|x-y|^{2s+d}}dy, \quad C_{d,2s} = 2^{2s}\frac{\Gamma\left(s + d/2\right)}{\pi^{d/2}|\Gamma(-s)|}, \quad 0 < s \leq 1. \tag{13}$$

In order to simplify the notation for the remainder of this paper, we write

$$-(-\Delta)^s \text{ as } \Delta^s. \tag{14}$$

Normalizing the operator by $C_{d,2s}$ leads to a simple form for Δ^s in Fourier space [20, 36, 12]

$$\mathcal{F}_{x\mapsto q}\left\{\Delta^s f(x)\right\} = -|q|^{2s}\mathcal{F}_{x\mapsto q}\{f(x)\}. \tag{15}$$

Note that the case $s = 1$ (i.e. $\mu = 3$ in one dimension) reduces to the usual Laplacian. We will use equation (15) both for the following numerical simulations and the stability analysis in Section 3.

For convenience, we define the parameter

$$s := \frac{\mu - 1}{2} \tag{16}$$

so that in one-dimension

$$l\mathcal{L}A_k \sim C_{1,2s}^{-1}\Delta^s(A)$$

and

$$\sum_{i\in\mathbb{Z},i\neq k} N_i(1 - A_i\delta t)q_{i\to k} - N_k \sim \frac{l^{\mu-1}}{z}C_{1,2s}^{-1}\left[A\Delta^s\left(\frac{N}{A}\right) - \frac{N}{A}\Delta^s\left(A\right)\right] - \delta t AN.$$

The continuum limit of (5) then becomes

$$\frac{\partial N}{\partial t} = \frac{l^{\mu-1}}{\delta t}\frac{\pi^{1/2}2^{1-\mu}|\Gamma\left(\frac{1-\mu}{2}\right)|}{z\Gamma\left(\mu\right)}\left[A\Delta^s\left(\frac{N}{A}\right) - \frac{N}{A}\Delta^s\left(A\right)\right] - AN + \Gamma. \tag{17}$$

Finally we rescale variables to eliminate the parameters w and θ from the equations as follows: $A = \bar{A}w, \quad N = \rho w/\theta, \ t = \bar{t}/w$. Dropping the bars, we obtain

$$\frac{\partial A}{\partial t} = \eta A_{xx} - A + \alpha + A\rho. \tag{18}$$

$$\frac{\partial \rho}{\partial t} = D\left[A\Delta^s\left(\frac{\rho}{A}\right) - \frac{\rho}{A}\Delta^s\left(A\right)\right] - A\rho + \beta \tag{19}$$

where

$$s = \frac{\mu - 1}{2} \in (0, 1], \ \eta = \frac{l^2\hat{\eta}}{2\delta t w}, \ D = \frac{l^{2s}}{\delta t}\frac{\pi^{1/2}2^{-2s}|\Gamma\left(-s\right)|}{z\Gamma\left(2s+1\right)w}, \ \alpha = \frac{A_0}{w}, \text{ and } \beta = \frac{\Gamma\theta}{w^2}. \tag{20}$$

To validate the continuum model, we perform direct numerical simulations of the agent-based model (1-5) and the continuum model (18, 19). Implementing the cellular automata model is straightforward: we consider a lattice of n points and set $A_k, B_k, N_k = 0$ whenever $k \notin \{1, \ldots, n\}$ in (1-5). Due to the nonlocal motion of criminals, each time step in the discrete model takes $O(n^2)$ time. For the continuum model, we employ a spectral method in space based on the Fast Fourier Transform (FFT) with the method of lines in time. We first discretize A and ρ in space using K meshpoints, then we solve the $2K$ coupled ordinary differential equations (ODEs) in time. To approximate $\Delta^s u$, we make use of property (15) in Fourier space. On the interval $x \in [0, L]$, this is done through the FFT, as illustrated in the following Matlab code,

```
K = numel(u); % u is a 1 by K array ;
q = 2*pi/L*[0:K/2-1, -K/2:-1];
laplaces_u = ifft(-abs(q).^(2*s).*fft(u));
```

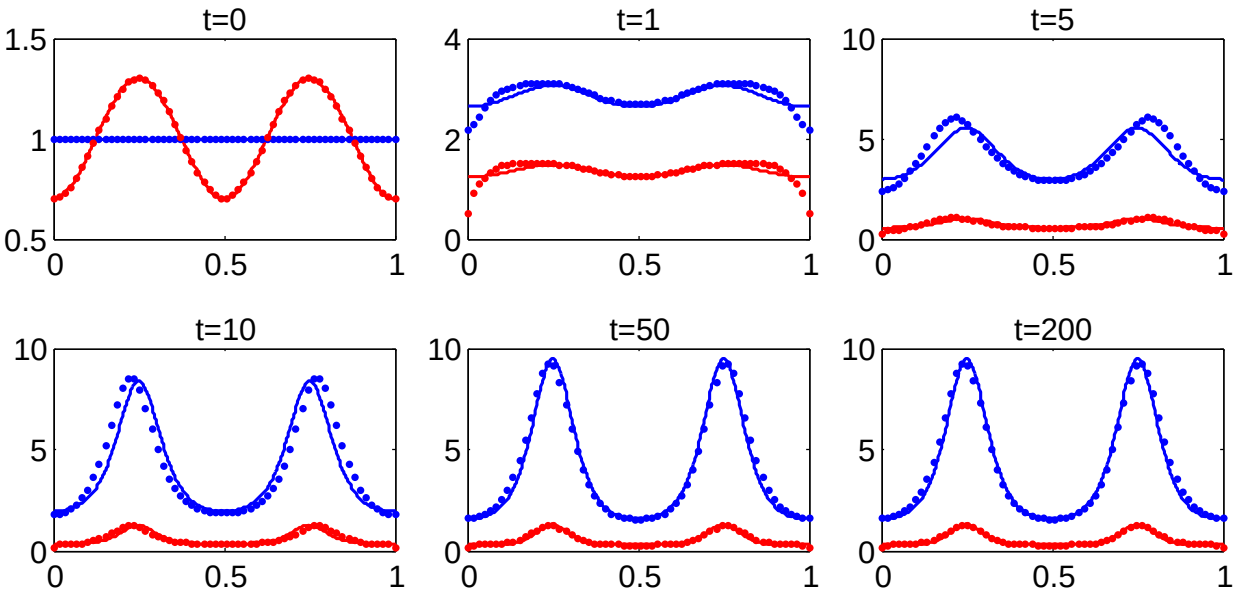

Figure 1: Simulations of a discrete model (1-5) and its continuum limit (18, 19). The discrete model is shown with blue dots (for A) and red crosses (for N). The continuum model is shown in blue and red curves for A and ρ, respectively. Parameters for the discrete model are: $\mu = 2.5$, $n = 60, l = 1/60$, $\hat{\eta} = 0.1$, $\delta t = 0.01$, $A_0 = 1$, $\Gamma = 3$. The corresponding parameters for the continuum model are computed from (20) as $s = 0.75, \eta = 0.001388, D = 0.1828, \alpha = 1, \beta = 3$.

The FFT enables us to calculate one time step in the continuum model in $O(K \log K)$ time, where K is the number of gridpoints in the discretization. This computation assumes periodic boundary conditions for the solution.

Figure 1 shows a comparison between the numerical simulations for the discrete and continuous model. Excellent agreement is observed away from the boundaries. Near the boundaries, some disagreement is expected as the discrete case was not performed with periodic boundary conditions (incorporating more realistic boundary conditions for the continuum model is discussed in [36] but is outside the scope of this paper). Eventually, the pattern settles into a steady-state consisting of two hotspots.

From (20), we find that $\eta^{-s} D = O((1-s)^{-1} (\delta t)^{s-1}) \gg 1$ for $0 < s \leq 1$ (the factor $(1-s)^{-1}$ comes from expanding $|\Gamma(-s)| \sim 1/(1-s)$ in the limit $s \to 1^-$). Thus, in the physically relevant regime $0 < s \leq 1$, the following condition holds:

$$\eta^{-s} D \gg 1; \quad 0 < s \leq 1. \tag{21}$$

In analogy with regular diffusion ($s = 1$), we refer to this condition as the "*separation of scales*"; it implies that the criminals ρ diffuse much faster than the activation field A, and plays a key role in the Turing analysis as well as the asymptotic construction of the hotspots below.

3 Turing instability

We now perform a linear Turing analysis around the homogeneous steady state of (18, 19) given by

$$\bar{A} = \alpha + \beta; \quad \bar{\rho} = \frac{\beta}{\alpha + \beta}. \tag{22}$$

Perturbing from the steady state (22), we write

$$A(x,t) = \overline{A} + \phi e^{\lambda t} e^{ikx}; \qquad \rho(x,t) = \overline{\rho} + \psi e^{\lambda t} e^{ikx}. \tag{23}$$

and look for a relationship between the different Fourier modes and the eigenvalues λ. Using equation (15), we have

$$\Delta^s e^{ikx} = -|k|^{2s} e^{ikx}$$

which yields the eigenvalue problem

$$\begin{bmatrix} -\eta|k|^2 - 1 + \bar{\rho} & \bar{A} \\ \frac{2\bar{\rho}}{\bar{A}} D|k|^{2s} - \bar{\rho} & -D|k|^{2s} - \bar{A} \end{bmatrix} \begin{bmatrix} \phi \\ \psi \end{bmatrix} = \lambda \begin{bmatrix} \phi \\ \psi \end{bmatrix}. \tag{24}$$

The dispersion relationship $\lambda = \lambda(k)$ is then given by

$$\lambda^2 - \tau\lambda + \delta = 0 \tag{25}$$

where

$$\tau = -D|k|^{2s} - \eta|k|^2 - \bar{A} - 1 + \bar{\rho} \quad \text{and} \quad \delta = D|k|^{2s}\left(\eta\,|k|^2 + 1 - 3\bar{\rho}\right) + \eta\,|k|^2\,\bar{A} + \bar{A}. \tag{26}$$

Figure 2 illustrates the effects of changing the strength of the Lévy walk decay exponent s on the stability of the homogeneous steady state. There are five distinct possible regimes labelled (a) through (e) in the figure.

To determine the stability of the steady state (22), first note that $\tau < 0$. This implies that the steady state is stable if $\delta > 0$. In particular, we have stability if $\bar{\rho} < 1/3$ (i.e. $\alpha > 2\beta$). On the other hand, an instability occurs if $\delta < 0$ or

$$\bar{A} < D|k|^{2s}\left(-1 + \frac{3\bar{\rho}}{\eta\,|k|^2 + 1}\right) \text{ for some } k. \tag{27}$$

By computing the maximum of the right hand side of this equation, we obtain the following characterization of the stability.

Proposition 3.1. *Suppose that $\alpha > 2\beta$(i.e. $\bar{\rho} < 1/3$). Then the homogeneous equilibrium (22) is stable. Suppose that $\bar{\rho} > 1/3$ and $A < A_*$ where*

$$\bar{A}_* := D\eta^s x^s\left(-1 + \frac{3\bar{\rho}}{x+1}\right) \tag{28}$$

and where x is the unique positive root of

$$x^2 + x\,(2 + 3\bar{\rho}(1-s)/s) + 1 - 3\bar{\rho} = 0. \tag{29}$$

Then the equilibrium (22) is unstable.

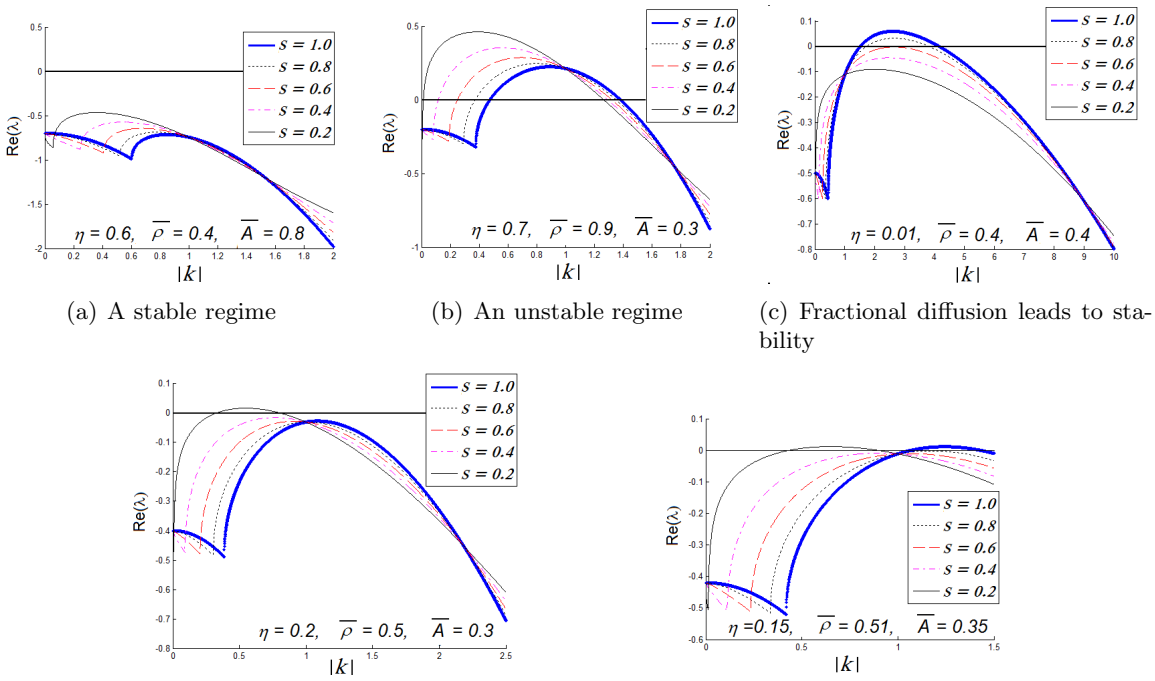

(a) A stable regime

(b) An unstable regime

(c) Fractional diffusion leads to stability

(d) Fractional diffusion leads to instability

(e) Fractional diffusion leads to stability and then instability

Figure 2: Different possible effects from fractional diffusion on the dispersion relation (25). A positive value for $\mathrm{Re}(\lambda)$ corresponds to an unstable homogeneous steady-state.

Note that the boundary between the stable and unstable steady state is is given by $A = A_*$. Figure 3 illustrates the predictive value of proposition 3.1. The dashed blue curve shows the boundary $A = A_*$ between instability and stability. The homogeneous steady state is stable above the curve, and unstable below it. The numerical simulations for the full non-local equation agree very well with the linear predictions; the exceptions plotted in red all lie very close to the bifurcation boundary.

We next concentrate on the physically relevant parameter regime $\eta^{-s} D \gg 1$ (see page 6). Equation (27) implies that the equilibrium (22) is unstable for all modes of order $k = O(\eta^{-1/2})$, provided that $\bar{\rho} > 1/3$ and $\bar{A}, \bar{\rho} = O(1)$. To compute the dominant unstable mode, we change variables $k = x^{1/2}\eta^{-1/2}$ and let $M = D\eta^{-s} \gg 1$. We then obtain

$$\tau = -Mx^s - x^2 + \bar{\rho} - 1 - \bar{A} \quad \text{and} \quad \delta = Mx^s(x + 1 - 3\bar{\rho}) + x\bar{A} + \bar{A}.$$

The fastest growing mode corresponds to the maximum of the dispersion curve, when $\lambda = \tau_x/\delta_x$. Substituting this into (25) we then obtain the following equation for x :

$$2(s+1)x^2 - 2s(s\bar{\rho} + \bar{A} + 4\bar{\rho} - 1)x + s^2\bar{\rho}(-2 + 3\bar{A} + 6\bar{\rho}) - Msx^{s+1} = 0. \tag{30}$$

This admits an asymptotic solution

$$x \sim \left[s\bar{\rho}(-2 + 3\bar{A} + 6\bar{\rho})M^{-1}\right]^{\frac{1}{s+1}}, \quad M \gg 1$$

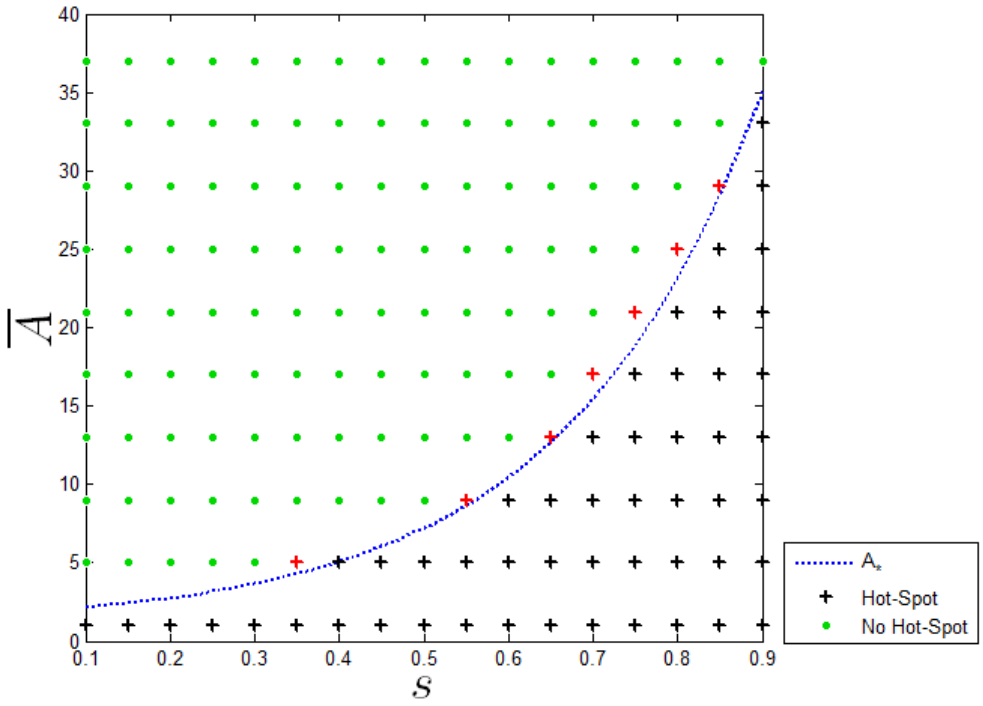

Figure 3: Comparison between the predicted instability threshold given by proposition 3.1 and direct numerical simulations of the continuum model (18, 19). Parameter values are $\eta = 0.001, \bar{\rho} = 1, D = 1$. Red marks denote inconsistencies between the two approaches.

so that

$$k_{\text{fastest}}(s) \sim \left[\frac{s\bar{\rho}(-2 + 3\bar{A} + 6\bar{\rho})}{D\eta}\right]^{\frac{1}{2(s+1)}}, \quad D\eta^{-s} \gg 1. \tag{31}$$

We summarize as follows.

Proposition 3.2. *Suppose that $D\eta^{-s} \gg 1$, with $\alpha, \beta = O(1)$. Then the homogeneous equilibrim (22) is stable if $\alpha > 2\beta$ and is unstable if $\alpha < 2\beta$. In the latter case, the most unstable mode is asymptotically given by (31).*

Formula (31) provides a way of obtaining a rough estimate of the total number of expected hotspots. Namely, on a domain of size L with periodic boundary conditions, an instability of the form (23) has $kL/(2\pi)$ maxima. If each of these maxima eventually forms a fully developed hotspot, then the total number of maxima from the perturbation (23) can be approximated as

$$\text{Expected number of maxima} \approx \text{floor}\left(\frac{L}{2\pi} k_{\text{fastest}}\right). \tag{32}$$

As is illustrated in figure 4, this typically over-predicts the final number of hotspots. Equation (32) relies on a linear analysis near the homogeneous equilibrium to predict the eventual number of hotspots. However, hotspots are localized patterns in the nonlinear regime far from the homogeneous equilibrium, and as such, there is no *a priori* reason to expect a Turing analysis to predict

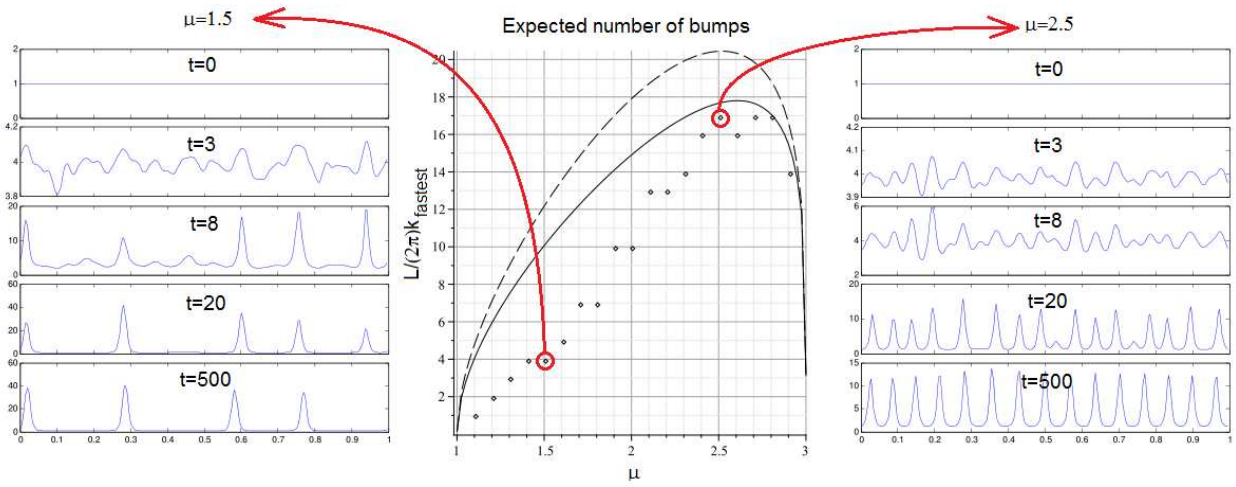

Figure 4: CENTER: Number of hotspots as a function of the Lévy walk decay exponent μ. The dashed curve represents the asymptotics as given by (31); the solid curve is the exact prediction from the dispersion relationship given by $k = x^{1/2}\eta^{-1/2}$ where x satisfies (30); the dots represent the observed number of hotspots from the full numerical simulation of the continuum model (18, 19). Parameter of the continuum model are as given by (20) with $L = 1$ and with $l = 0.01, \delta t = 0.05, \hat{\eta} = 0.02,\ A_0 = 1, \Gamma = 3, w = \theta = 1$. LEFT: Snapshots of the simulation of the continuum model starting with small random fluctuations about the steady state. Initially, around 11 "bumps" form at $t = 3$. However, eventually only four hotspots are left at $t = 500$ due to a coarsening process. RIGHT: Simulations with $\mu = 2.5$. Unlike the figure on the left, the inital number of "bumps" is similar to the eventual number of hotspots.

the eventual number of hotspots. Nonetheless as figure 4 illustrates, the Turing analysis appears to provide an upper bound for the number of stable hotspots in the nonlinear regime.

In terms of the model's original parameters, the dominant unstable mode (31) can be written as

$$k_{\text{fastest}}(\mu) \sim \frac{1}{l}\left[\frac{1}{|\Gamma\left(\frac{1-\mu}{2}\right)|}\left\{\frac{(\mu-1)\,\Gamma(\mu)\,\bar{\rho}(-2+3\bar{A}+6\bar{\rho})zw^2\,(\delta t)^2}{\hat{\eta}\pi^{1/2}2^{1-\mu}}\right\}\right]^{\frac{1}{\mu+1}}.$$

Note that the term in curly braces is $O((\delta t)^2) \ll 1$. Because of this, the maximum of this function is attained near $\mu \sim 3$. This is seen by expanding $|\Gamma\left(\frac{1-\mu}{2}\right)| \sim 2/(3-\mu)$ as $\mu \to 3^-$. We then obtain

$$k_{\text{fastest}}(\mu) \sim \frac{1}{l}\left[(3-\mu)\varepsilon\right]^{\frac{1}{\mu+1}};\quad \text{where}\quad \varepsilon := (\delta t)^2\,\frac{8\bar{\rho}(-2+3\bar{A}+6\bar{\rho})zw^2}{\hat{\eta}\pi^{1/2}};\quad 0 < 3-\mu \ll 1. \tag{33}$$

The maximum of (33) is at $\mu_{\text{optimal}} \sim 3 - x$ where x satisfies the transcendental equation

$$x = \frac{4}{1+\ln\frac{1}{\varepsilon x}}.$$

To leading order, we therefore obtain

$$\mu_{\text{optimal}} \sim 3 - \frac{2}{\ln(1/\delta t)}. \tag{34}$$

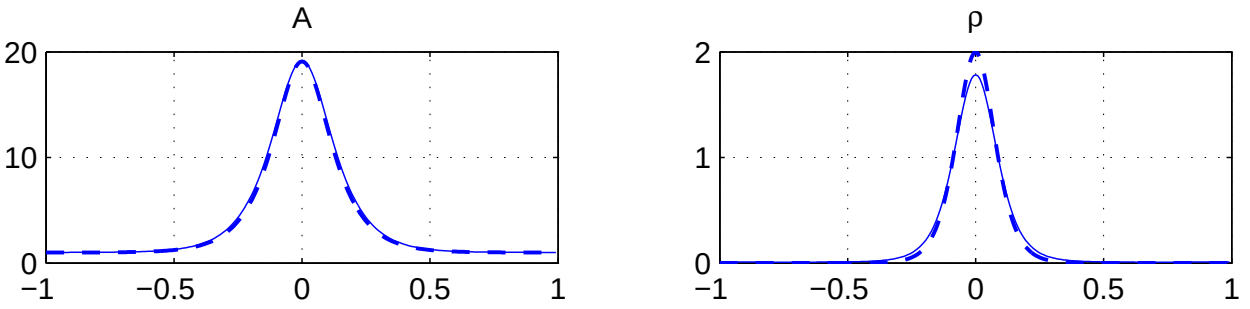

Figure 5: A single hotspot equilibrium solution to (35) for parameter values $s = 0.5, \eta = 0.01, D = 1/\eta, \beta = 3$, $\alpha = 1, L = 1$. The solid curve shows the full numerical simulations of the continuum model (18, 19). The dashed line shows the asymptotic approximation for A and ρ as derived in proposition 4.1.

4 Asymptotic hotspot profile

As figure 4 illustrates, a Turing instability often leads to the formation of localized pulses, herein referred to as hotspots, rather than dispersion-type waves. In the singular limit where the diffusion of attractiveness is much less than the diffusion of criminals, the profile of the localized pulse can be understood. The profile and stability of these spots was studied in [19] for the standard diffusion case $s = 1$. Here, we generalize the basic construction of the hotspot performed in [19] to our Lévy flight model; the stability of these pulses is left for future work. We seek a symmetric steady state on the domain $[-L, L]$ in the form of a single spike centered at zero. The desired solution is illustrated in figure 5. Such steady states on the domain $x \in [-L, L]$ satisfy

$$\begin{aligned} 0 &= \eta A_{xx} - A + \alpha + A\rho \\ 0 &= D\left[A\Delta^s\left(\frac{\rho}{A}\right) - \frac{\rho}{A}\Delta^s(A)\right] - A\rho + \beta, \end{aligned} \tag{35}$$

with the additional conditions

$$A(x) = A(-x), \quad \text{and} \quad \rho(x) = \rho(-x).$$

First, we concentrate on the inner region, near $x = 0$, at the interior of the spike. Changing into the variable

$$x = \sqrt{\eta} y$$

we find

$$0 = A_{yy} - A + \alpha + A\rho, \qquad 0 = D\eta^{-s}\left[A\Delta_y^s\left(\frac{\rho}{A}\right) - \frac{\rho}{A}\Delta_y^s(A)\right] - A\rho + \beta.$$

We recall that the assumption on the relative diffusion of attractiveness and criminals implies

$$D\eta^{-s} \gg 1.$$

Then the leading order terms in (35) yield

$$A\Delta_y^s\left(\frac{\rho}{A}\right) - \frac{\rho}{A}\Delta_y^s(A) \sim 0.$$

This equation has solution

$$\rho = v_0 A^2$$

where v_0 is still to be determined. The inner problem becomes

$$0 \sim A_{yy} - A + \alpha + A^3 v_0.$$

The self-consistent ansatz

$$v_0 = O(\eta) \ll 1$$

follows from the following computations. Assuming that $\alpha = O(1)$, we then have

$$A(y) \sim v_0^{-1/2} w(y)$$

where w satisfies the ground state equation

$$w_{yy} - w + w^3 = 0, \quad w \to 0 \text{ as } |y| \to \infty, \quad w'(0) = 0.$$

This ground state has a well-known homoclinic orbit which can be computed explicitly as

$$w(y) = \sqrt{2}\,\mathrm{sech}(y).$$

It remains to determine v_0. To do so, we integrate the second equation in (35). For any two functions u, v, note that

$$\int \left[u\Delta^s(v) - v\Delta^s(u)\right] dx = C \int\int \frac{u(x)\left(v(y) - v(x)\right) - v(x)\left(u(y) - u(x)\right)}{|x-y|^{2s+1}} dxdy = 0$$

so we obtain

$$\int_0^L A\rho dx = \int_0^L \beta dx = \beta L.$$

To estimate the left hand side, we make the assumption that $A\rho \ll 1$ in the outer region away from the spike. This leads to

$$\begin{aligned}\int_0^L A\rho dx &\sim \int_0^\infty A^3(y) v_0 \eta^{1/2} dy \sim \eta^{1/2} v_0^{-1/2} \int_0^\infty w^3 dy \\ &\sim \eta^{1/2} v_0^{-1/2} \pi/\sqrt{2}\end{aligned}$$

which yields

$$v_0^{-1/2} \sim 2^{1/2} \beta L \eta^{-1/2}/\pi. \tag{36}$$

To verify the assumption that $A\rho \ll 1$, we again change variables

$$\rho = vA^2$$

with $v(0) = v_0$. Then (35) becomes

$$D\left[A\Delta^s(Av) - Av\Delta^s(A)\right] - A^3 v + \beta = 0 = \eta A_{xx} - A + \alpha + A^3 v. \tag{37}$$

To be self-consistent, we need $A^3 v \ll O(1)$ in the outer region. Then $A \sim \alpha = O(1)$ such that in the outer region we obtain

$$D\Delta^s v - \alpha v + \beta/\alpha^2 \sim 0.$$

From (36), note that $v_0 = O(\eta)$; this suggests a rescaling $v = \hat{v}\eta$ in the outer region giving $D\eta\Delta^s\hat{v} + \beta/\alpha^2 \sim 0$ with $\hat{v}(0) = 2^{1/2}\beta L/\pi = O(1)$. It follows that if $D\eta \geq O(1)$, then $\hat{v} = 0(1)$ and we find $A^3 v = O(\eta) \ll O(1)$ as desired. In conclusion, the self-consistency condition is precisely $D\eta \geq O(1)$. We summarize as follows.

Proposition 4.1. *Consider a single hotspot on the interval $[-L, L]$. Suppose that $D\eta^{-s} \gg 1$ and $D\eta \geq O(1)$, with $\alpha, \beta = O(1)$. Then the spike profile in the inner region satisfies*

$$A \sim \frac{2}{\pi}\beta L\eta^{-1/2}\,\mathrm{sech}(x\eta^{-1/2}), \qquad |x| \leq O(\eta^{1/2}) \tag{38}$$

$$\rho \sim 2\,\mathrm{sech}^2(x\eta^{-1/2}). \tag{39}$$

In the outer region $|x| \gg O(\eta^{1/2})$, we have $A \sim \alpha$.

Note that a solution for A that is uniformly valid in both the inner and outer regions is

$$A \sim (\frac{2}{\pi}\beta L\eta^{-1/2} - \alpha)\,\mathrm{sech}(x\eta^{-1/2}) + \alpha. \tag{40}$$

A sample verification of Proposition 4.1 is displayed in figure 5: the asymptotic expression (40, 39) is compared to the numerically computed steady state with good agreement.

5 Discussion

As seen in figure 4, there is an optimal value of the Lévy flight exponent $\mu_{\text{optimal}} \in (1, 3]$ which leads to the largest number of hotspots. From a criminal's point of view, such an optimal exponent might lead to the best chance of successfully burgling a house. The amplitude of the attractiveness for the hotspots varies with the total number of hotspots. This means sites may drop in attractiveness, and in some sense criminal payoff, if there are a large number of hotspots. However, if there are more attractive burglary sites, then there is a larger area to patrol, and a smaller likelihood that the police will intervene at any single location. Intuitively, if the criminals move too sporadically (smaller μ), they will miss some opportunities for looting. As μ decreases, the biased Lévy flight make it more likely that the criminals jump from one hotspot to another. The total number of hotspots will be small with large amplitudes, and the criminals will be concentrated in a few tiny regions. On the other hand, they will also miss opportunities if they move very little. The best strategy should therefore be a compromise between widely ranging the state space and exploring localized niches. Note that the optimal value of $\mu_{\text{optimal}} \sim 3 - \frac{2}{\ln(1/\delta t)}$ as computed in (34) is relatively close to a random walk and Brownian motion $\mu = 3$.

The physical constraints of the model naturally lead to the *separation of scales* $\eta^{-s}D \gg 1$ in the continuum model (see page 6). This same condition naturally arises in the asymptotic construction of the hotspot (proposition 4.1). Additionally, this condition is necessary in proposition 3.2 which provides a sharp threshold boundary $\alpha \sim 2\beta$ for the Turing instability. Under the natural assumption $\eta^{-s}D \gg 1$, it is expected that the hotspot solutions will co-exist with dispersion-type waves when $\alpha < 2\beta$. In particular, we expect a subcritical bifurcation of the homogeneous steady state at the bifurcation point as $\alpha \to 2\beta$ from below. This observation is consistent with the analysis in [19] (see figure 7 therein) as well as the weakly nonlinear analysis in [27] for the standard diffusion case $s = 1$.

While this paper concentrates on one dimensional hotspots, we have also performed numerical simulations in two dimensions for the cellular automata model to see the effect of a biased Lévy flight. These simulations indicate that similarly to the one dimensional case, the amplitude and number of hotspots varies with the exponent μ.

Lévy flights crucially produce fractional Laplacians in the continuous limit. Fractional Laplacians have a particularly simple Fourier Transform (15) which makes it possible to efficiently solve the corresponding non-local partial differential equations numerically through the FFT. This property also enables an analytical computation of the Turing instability. It would be interesting to generalize the computations of this paper to more realistic models of human locomotion [11, 24, 6]. In [11, 24], it is suggested that the spatial step sizes are distributed according to a truncated Lévy Flight with an inner cutoff radius near the origin where the steps are uniformly distributed, and an outer cutoff radius where the step sizes are exponentially distributed; the power law distribution is observed in between the two radial cutoffs. Such a model is easy to implement in the cellular automata model: the weights (3) are replaced with $w_{i\to k} = A_k f(l|i-k|)$ where

$$f(r) = \begin{cases} 1, & r < r_1 \\ (r/r_1)^{-\mu}, & r_1 < r < r_2 \\ (r_2/r_1)^{-\mu} \exp(-(r-r_2)\,\nu), & r > r_2 \end{cases}$$

and r_1,r_2 $\mu, \nu > 0$ are appropriately chosen parameters. Unfortunately, such a choice of $f(r)$ does not have a simple expression for its Fourier transform which makes it harder to analyze. Nonetheless, our formulation of the biased walk can be extended to more general models and more realistic spatial networks. Moreover, we expect that the leading order asymptotic construction of the hotspot profile will not depend on the precise form of $f(r)$.

As shown in figure 4, the Turing instability does not predict the eventual number of hotspots. These structures are in the fully nonlinear regime and are typically far from the Turing instability threshold. Instead, the stability theory for spike-type solutions as developed in [13] needs to be extended to the non-local case. For the original model with a biased Brownian motion of criminals, this has been done in [19]. Extending the theory to biased Lévy flights remains an open question.

6 Acknowledgments

We thank Andrea Bertozzi for fruitful discussions and suggestions. This work was supported by the California Research Training Program in Computational and Applied Mathematics (NSF grant DMS-1045536). SC was supported in part by Harvey Mudd College and additionally by the Royal Thai Government through a Royal Thai Scholarship from the Development and Promotion of Science and Technology Talents Project (DPST). JB and DY were funded by NSF grant DMS-1045536. TK was supported by a grant from AARMS CRG in Dynamical Systems and NSERC grant 47050. SGM was supported by ARO MURI grant W911NF-11-1-0332, and this work was additionally supported by ARO grant W911NF1010472 and NSF grant DMS-0968309.

References

[1] D. Beavon, P.L. Brantingham, and P.J. Brantingham. *Crime Prevention Studies*. Willow Tree Press, 1994.

[2] Wim Bernasco and Paul Nieuwbeerta. How do residential burglars select target areas?: A new approach to the analysis of criminal location choice. *British Journal of Criminology*, 45(3):296–315, May 2005.

[3] A. E. Bottoms and P. Wiles. *Crime, Policing And Place: Essays in Environmental Criminology*. Routledge, 1992.

[4] Patricia Brantingham and Paul Brantingham. Criminality of place. *European Journal on Criminal Policy and Research*, 3:5–26, 1995. 10.1007/BF02242925.

[5] P.J. Brantingham and P.L. Brantingham. *Patterns in Crime*. Macmillan, 1984.

[6] D. Brockmann, Hufnagel D., L., and T. Geisel. The scaling laws of human travel. *Nature*, 439:462–465, 2006.

[7] J.E. Eck, S. Chainey, J.G. Cameron, M. Leitner, and R.E. Wilson. Mapping crime: understanding hot spots. 2005.

[8] G Farrell and K (ads) Pease. *Repeat victimization*. Criminal Justice Press, Monsey, 2001.

[9] Graham Farrell, Coretta Phillips, and Ken Pease. Like taking candy - why does repeat victimization occur. *Brit. J. Criminology*, 35:384, 1995.

[10] M.K. Felson. *Crime and Nature*. Sage Publications, 2006.

[11] M. C. Gonzalez, C. A. Hidalgo, and A. L. Barabasi. Understanding individual human mobility patterns, Nature. 453:779–782, June 2008.

[12] Barry D. Hughes, Michael F. Shlesinger, and Elliott W. Montroll. Random walks with self-similar clusters. *Proceedings of the National Academy of Sciences*, 78(6):3287–3291, 1981.

[13] D. Iron, M. J. Ward, and J. Wei. The stability of spike solutions to the one-dimensional Gierer–Meinhardt model. *Physica D*, 150(1-2), 2001.

[14] Alex James, Michael J. Plank, and Andrew M. Edwards. Assessing Lévy walks as models of animal foraging. *Journal of The Royal Society Interface*, 8(62):1233–1247, 2011.

[15] S. D. JOHNSON, K. BOWERS, and A. HIRSCHFIELD. New insights into the spatial and temporal distribution of repeat victimization. *British Journal of Criminology*, 37(2):224–241, 1997.

[16] Shane Johnson. Repeat burglary victimisation: a tale of two theories. *Journal of Experimental Criminology*, 4:215–240, 2008. 10.1007/s11292-008-9055-3.

[17] Shane Johnson, Wim Bernasco, Kate Bowers, Henk Elffers, Jerry Ratcliffe, George Rengert, and Michael Townsley. Space-time patterns of risk: A cross national assessment of residential burglary victimization. *Journal of Quantitative Criminology*, 23:201–219, 2007. 10.1007/s10940-007-9025-3.

[18] Shane D. Johnson and Kate J. Bowers. The stability of space-time clusters of burglary. *British Journal of Criminology*, 44(1):55–65, 2004.

[19] T. Kolokolnikov, M. Ward, and J. Wei. The Stability of Steady-State Hot-Spot Patterns for a Reaction-Diffusion Model of Urban Crime. *ArXiv e-prints*, January 2012.

[20] Y. Nec. Spike-type solutions to one dimensional Gierer–Meinhardt model with Lévy flights. *Studies in Applied Mathematics*, pages no–no, 2012.

[21] J. H. Ratcliffe and M. J. McCullagh. Hotbeds of crime and the search for spatial accuracy. *Journal of Geographical Systems*, 1:385–398, 1999. 10.1007/s101090050020.

[22] J. H. Ratcliffe and George F Rengert. Near-repeat patterns in philadelphia shootings. *Security Journal*, 21:58–76, 2008.

[23] G.F. Rengert. *Crime, Policing And Place: Essays in Environmental Criminology*. Routledge, 1992.

[24] Injong Rhee, Minsu Shin, Seongik Hong, Kyunghan Lee, Seong Joon Kim, and Song Chong. On the Lévy-walk nature of human mobility. *IEEE/ACM Trans. Netw.*, 19(3):630–643, June 2011.

[25] Dennis W. Roncek and Ralph Bell. Bars, blocks, and crimes. *Journal of Environmental Systems*, 11, 1981.

[26] Alex Sagovsky and Shane D. Johnson. When does repeat burglary victimisation occur? *Australian and New Zealand Journal of Criminology*, 40(1):1–26, 2007.

[27] M. B. Short, A. L. Bertozzi, and P. J. Brantingham. Nonlinear patterns in urban crime - hotspots, bifurcations, and suppression. *SIAM J. Appl. Dyn. Sys.*, 9(2):462–483, 2010.

[28] M. B. Short, M. R. D'Orsogna, V. B. Pasour, G. E. Tita, P. J. Brantingham, A. L. Bertozzi, and L. B. Chayes. A statistical model of criminal behavior. *Mathematical Models and Methods in Applied Sciences*, 18:1249 – 1267, 2008.

[29] M.B. Short, P.J. Brantingham, A.L. Bertozzi, and G.E. Tita. Dissipation and displacement of hotspots in reaction-diffusion models of crime. *Proceedings of the National Academy of Sciences of the United States of America*, 107:3961–3965, 2010.

[30] M.B. Short, M. D'Orsogna, P.J. Brantingham, and G.E. Tita. Measuring and modeling repeat and near-repeat burglary effects. *Journal of Quantitative Criminology*, 25:325–339, 2009. 10.1007/s10940-009-9068-8.

[31] Michael Townsley, Ross Homel, and Janet Chaseling. Infectious burglaries. a test of the near repeat hypothesis. *British Journal of Criminology*, 43(3):615–633, 2003.

[32] Andromachi Tseloni and Ken Pease. Repeat personal victimization. boosts or flags? *British Journal of Criminology*, 43(1):196–212, 2003.

[33] Andromachi Tseloni and Ken Pease. Repeat personal victimization: Random effects, event dependence and unexplained heterogeneity. *British Journal of Criminology*, 44(6):931–945, 2004.

[34] J. Q. Wilson and G. L. Kelling. Broken windows and police and neighborhood safety. *Atlantic Mon.*, 249:29–38, 1982.

[35] R. Wright and S. Decker. *Burglars on the Job*. Northeastern University Press, 1994.

[36] A. Zoia, A. Rosso, and M. Kardar. Fractional laplacian in bounded domains. *Phys. Rev. E*, 76:021116, Aug 2007.